Scene Illuminant Estimation of Multiple Light Sources

Shoji Tominaga, Takahiko Horiuchi and Yu Kato
Graduate School of Advanced Integration Science, Chiba University, Chiba, Japan

Abstract

This paper proposes a method for estimating the illuminant spectral power distributions and their relative positional relationship of multiple light sources under a complex illumination environment. A multiband camera system is used for capturing spectral images of dielectric objects in a scene. First, dielectric object surfaces are segmented into regions with different object colors, by using the hue angle of the diffuse reflection component. Specular highlights are used as a clue for estimating the light source information, which are detected on curved object surfaces with the different object colors. The illuminant spectra of light sources are estimated from the camera data for highlight areas detected on each surface region. Then, the illuminant spectral estimates are obtained for a different set of light sources. Next, the geometric information, such as the number of light sources and their relative positional relationship is predicted based on the set of estimated illuminant spectra on the segmented surface regions. The algorithm of probabilistic relaxation labeling is used for classification of the detected highlights and the estimated spectra. The feasibility of the proposed method is examined in experiments on real scenes.

Introduction

Estimation of scene illumination from image data has important imaging applications, including image science and technology, computer vision, and computer graphics. The scene illuminant estimation problem has a long history. Although, so far, many methods were proposed for scene illuminant estimation, most methods assumed uniform illumination from a single light source [1]-[3]. We note that many illumination sources are present in natural scenes. The case of one source seldom happens. For example, Figure 1 illustrates an indoor scene having electric light sources of ceiling lamps, table lamps, and natural light source through windows. An outdoor scene may have the direct illumination source of sunlight and the second source of blue sky.

The problem of estimating multiple light sources has been discussed in the field of computer vision and computer graphics [4]-[6]. However, the purpose is not to estimate the illuminant spectral information, but to estimate the geometric information, such as the number, direction, and intensity of light sources. Moreover, most previous methods required images of a calibration object given shape (typically sphere), which needs to be removed from the scene and might cause artifacts. Recently, a methodology was presented for color constancy under multiple light sources, where a scene image was assumed to be captured under only one or two distinct light sources [7].

The present paper proposes a method for the detection and estimation of multiple illuminants, using only one multiband image of a scene under a complex illumination environment. Our method does not rely on object of fixed shape, but can be used on inhomogeneous dielectric objects of arbitrary convex shape. The most common light sources are point light sources, directional light sources, and area light sources. Specular highlights appearing on the object surfaces are used as a clue for estimating the light source information. We will estimate not only the illuminant spectral-power distributions of the light sources, but also predict the geometric information, such as the number of light sources and their relative positional relationship.

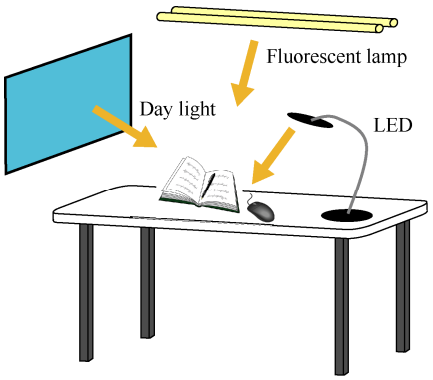

Figure 1. *Example of indoor natural scene.*

A multiband camera system is constructed for capturing spectral images. First, the image of object surfaces is segmented into uniform object color regions, by the diffuse reflection component of the dichromatic reflection model. Specular highlights are detected on the curved object surfaces with the different object colors. Then, the illuminant spectra of light sources are estimated from the multiband camera data for highlight areas detected on each surface region. Next, the geometric information of the number of light sources and their relative positional relationship is predicted based on the set of estimated illuminant spectra on the segmented surface regions, by using the algorithm of probabilistic relaxation labeling. Finally, we examine the feasibility of the proposed method in experiments on real scenes.

Imaging System

Figure 2 shows our multiband imaging system for capturing the high-dimensional spectral images. This system is realized using a liquid-crystal tunable (LCT) filter, a monochrome CCD camera with Peltier cooling system, and a personal computer. We represent illuminant spectra with 61-dimensional (61-D) vectors, where the visible wavelength range [400-700nm] is sampled at equal intervals of 5nm. The total spectral sensitivity functions of the imaging system are computed by using transmittance and the camera sensitivity the filter function, and the exposure time.

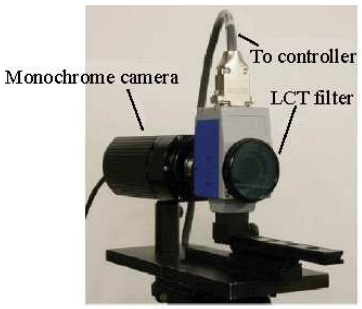

(a) System overview

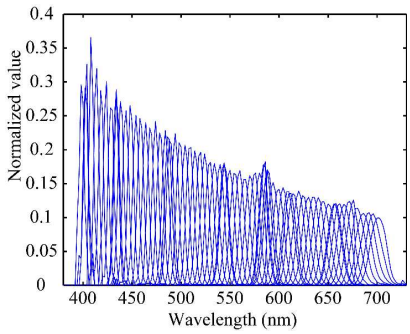

(b) Total spectral-sensitivity functions.

Figure 2. *Multi-band imaging system.*

Highlight Detection and Illuminant Spectral Estimation

Dichromatic Reflection Model

We assume that an object surface is composed of inhomogeneous dielectric material such as plastic or paint. The dichromatic reflection model suggests that light reflected from the object is decomposed into two additive components: specular and diffuse reflection components. Therefore, the radiance of the reflected light $Y(\theta, \lambda)$ is a function of the wavelength λ, ranging over the visible wavelengths, and the geometric parameter θ, which includes the all angles of incidence, phase, and viewing. This model describes the reflected light in the form

$$Y(\theta,\lambda) = c_S(\theta)E(\lambda) + c_D(\theta)S(\lambda)E(\lambda), \quad (1)$$

where $E(\lambda)$ and $S(\lambda)$ denote the spectral-power distribution of the incident light and the surface spectral reflectance of the object, respectively. The weights c_S and c_D are the geometrical scale factors. The specular reflection component indicated by the first term in Eq.(1) corresponds to the light-source color, and the diffuse reflection component indicated by the second term corresponds to the object color.

Detection of Object Color Regions and Highlight Areas

When a convex object surface is illuminated by several light sources from different directions, each of highlight areas is used as a clue for estimating the light sources because of the dichromatic reflection property.

Let $I(\lambda)$ be the observed color signal (radiance of the reflected light) from an object surface at each pixel point. The color signals can be recovered from the outputs of the multiband imaging system by knowing the spectral sensitivity functions $\{R_k(\lambda)\}$. First we compute the luminance value Y of the color signals as

$$Y = \int_{400}^{700} I(\lambda)\bar{y}(\lambda)d\lambda, \quad (2)$$

where $\bar{y}(\lambda)$ is the CIE luminosity function. A simple way for detecting highlight areas is to use a luminance threshold $Y \geq Y_0$ for the whole image area. However, highlight areas on different color objects cannot be detected appropriately by such a simple thresholding.

Therefore, in this paper, dielectric object surfaces are first segmented into regions with different object colors, by using the hue angle of the diffuse reflection component. The (x, y) chromaticity coordinates at each pixel are computed from the tristimulus values. Then we define the hue angle H as

$$H = \arctan(y - y_0, x - x_0), \quad (3)$$

where (x_0, y_0) is a standard white coordinates. Because most illuminants in a natural scene are approximated by the black-body radiator, the chromaticity coordinates are placed on the black-body locus on the xy diagram. We have found that the center coordinates of daylight black-body radiators are located closely to (1/3, 1/3). So we use normally $(x_0, y_0) = (1/3, 1/3)$.

We note that precise object segmentation is not necessary for the present illuminant estimation, but prominent highlights are necessary to be detected and classified into each object surface. In this paper, highlight areas are detected in two steps. First, different object color areas are segmented simply by the hue component. Although precise region segmentation may not be performed by the hue component, several regions with uniform colors are roughly extracted. Second, highlight areas are detected from the respective color area by using the luminance thresholding. Here, the luminance threshold is adaptively determined as $Y \geq Y_0^{(color\ area)}$. Thus, object color regions are detected from the image data and specular highlights are extracted on the curved object surfaces with the different object colors.

Estimation of Spectral-Power Distributions

Considering the dichromatic reflection property, the image data belonging to each detected highlight area are projected onto a 2-D space using two principal components as

$$\begin{bmatrix} C_1 \\ C_2 \end{bmatrix} = \begin{bmatrix} \mathbf{p}_1^t \\ \mathbf{p}_2^t \end{bmatrix} \mathbf{I}, \quad (4)$$

where $\mathbf{I}$ denotes the 61-D column vector representing the color signal, and $\mathbf{p}_1$ and $\mathbf{p}_2$ denote the first and second principal component vectors, which are computed from the image data set $\{\mathbf{I}\}$ belonging to the highlight area. A histogram of the projected 2-D image data (C_1, C_2) consists of two clusters for the specular reflection component and the diffuse reflection component according to the dichromatic reflection model. Figure 3 shows an example of the pixel distribution at a highlight area projected on (C_1, C_2) plane. Note that the histogram is divided into two linear clusters. Then, the cluster of specular reflection component indicating the light-source color is extracted to estimate illuminant.

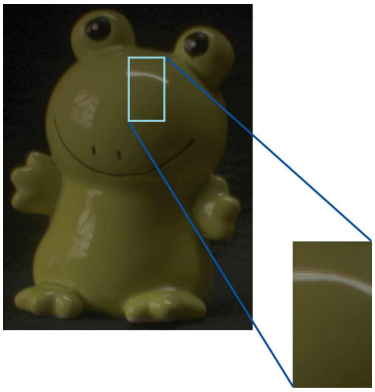

(a) An example of highlight area

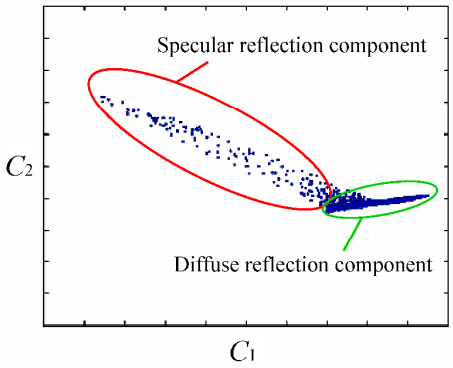

(b) 2-D pixel distribution

Figure 3. *2-D pixel distribution at a highlight area projected on (C_1, C_2) plane.*

It should be noted that the linear highlight cluster is much longer than the linear cluster of the diffuse reflection component. In this case, the principal component vector of the highlight cluster corresponds to the directional vector representing the illuminant. Therefore, both clusters are separated by an iterative optimization method, and the illuminant spectral-power distribution can be estimated by extracting the principal component vector of the highlight cluster and transforming it inversely into the original 61-D spectral space.

The estimated illuminant $\hat{\mathbf{e}}$ is calculated with the first principal component vector $(\hat{C}_1, \hat{C}_2)$ extracted from the highlight cluster as follows:

$$\hat{\mathbf{e}} = \hat{C}_1 \mathbf{p}_1 + \hat{C}_2 \mathbf{p}_2 , \tag{5}$$

Applying the above algorithm to the data for each highlight area provides a set of the estimated illuminant spectra for different light sources on each segmented object surface.

Estimation of Geometric Information of Light Sources

After the illuminant spectral estimation, the geometric information of the number of light sources and their relative positional relationship is predicted based on the set of estimated illuminant spectra and the detected highlight locations. The algorithm of probabilistic relaxation labeling [8] is used for classification of the candidate light sources.

Let label L_k be the k-th highlight on a reference object that has the most highlights among all the objects. All highlights on other objects are matched to the highlights on the reference object. Let O_i be the i-th highlight on another object. The detection of the relative positional relationship involves finding the most matched highlight label L_{k^*} on the reference object for all highlights $\{O_i\}$ on the other object. The probabilistic relaxation gives highlight O_i a probability $P_{i,k}$, $\left(\sum_k P_{i,k} = 1\right)$ for each label L_k on the reference object. Figure 4 shows an example of the notation for estimating the positional relationship among the light sources. In the figure, $P_{1,3}$ shows the probability which the highlight O_1 matches with the highlight L_3.

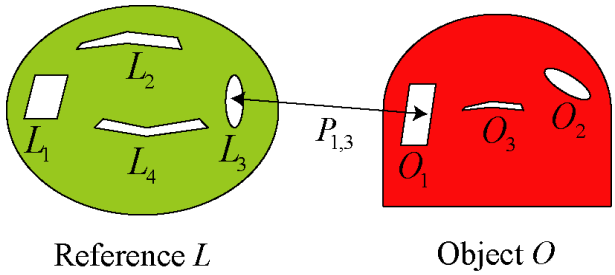

Figure 4. *Notation for estimating the positional relationship among the light sources.*

A candidate label, L_{k^*}, with the maximum probability is assigned as the final corresponding highlight for highlight O_i. The initial probabilities $P_{i,k}^{(0)}$ are derived from the root mean squared error, $\left\|\hat{\mathbf{e}}_i - \hat{\mathbf{e}}_k\right\|^{1/2}$, of the estimated spectral-power distributions between L_k and O_i. Then, the iterative processing is started and the probabilities are updated by the following iterative equation:

$$P_{i,k}^{(t+1)} = \frac{P_{i,k}^{(t)} \times q_{i,k}^{(t)}}{\sum_{k'} \left(P_{i,k'}^{(t)} \times q_{i,k'}^{(t)} \right)} . \tag{6}$$

The compatibility function (CF) denotes the contribution from the other highlights, which are defined as follows:

$$q_{i,k}^{(t)} = \sum_j \left\{ \max_l \left(r_{i,j,k,l} \times P_{j,l}^{(t)} \right) \right\} , \tag{7}$$

where L_l and O_j are the labels for highlight l on the reference object and highlight j on another object, respectively. The CF evaluates only the candidate label with the maximum probability. Compatibility coefficients, r, are formulated as follows:

$$r_{i,j,k,l} = \max\left(0,\ \alpha - \Delta deg_{i,j,k,l}\right),\ (\alpha > 0) , \tag{8}$$

where Δdeg indicates the spatial relationship between a pair of target highlights $\{L_k, O_i\}$ and another pair of highlights $\{L_l, O_j\}$ as shown in Fig. 5.

The iterative process is converged if the following condition is satisfied,

$$\left| \max_k P_{i,k}^{(t+1)} - \max_k P_{i,k}^{(t)} \right| < Th,\ \ \forall O_i , \tag{9}$$

where Th means a threshold of the convergence condition. Then, the label L_{k^*} with the maximum probability $P_{i,k^*}^{(t)}$ is assigned as the final corresponding highlight for highlight O_i.

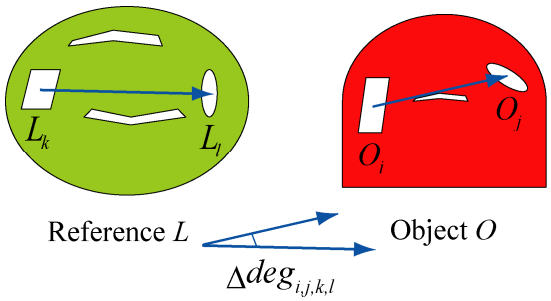

Figure 5. *Notation of the spatial relationship Δdeg between a pair of target highlights.*

After performing the above computational process for all objects, a set of corresponding highlights on all objects is determined for each label highlight L_k on the reference object. Finally, the number of the label highlight on the reference object becomes the number of light sources. The relative positional relationship can be derived from the geometric relations of label highlights on the reference object.

Experimental Results

Figure 6 shows an experimental scene. Plastic and ceramic objects placed on a table are illuminated using four different light sources: (1) daylight through the window, (2) a three-band fluorescent lamp, (3) an LED source, and (4) a three-band fluorescent lamp. The fluorescent lamps, (2) and (4), have the same spectral-power distribution.

Figure 7 shows the captured image of the four objects under the different illuminations. Figure 8 shows the highlight areas detected by the algorithm proposed in Sec. 3.2. Now let us check the details of the estimation results on the blue ceramic cup and the green object. Figures 9 and 10 show the spectral-power distributions estimated by the algorithm proposed in Sec. 3.3. The blue dotted curves show the estimated illuminant spectra, and the red curves show the direct measurements by using a spectro-radiometer. These results suggest a very high estimation accuracy of illuminant spectral-power distributions, including the spike peaks of the artificial illuminants of LED and fluorescence. As the result, we know that there are maximum four light sources with different three spectral distributions in the scene.

The proposed estimation of the spectral-power distribution is robust for even if the highlights fall near the border of a segmented area. However, the proposed algorithm does not work if almost superimposed plural lights exist in a detected highlight area.

Figure 11 shows the classification results for the light sources labeled by the probabilistic relaxation algorithm proposed in Sec. 3.4. The colored squares indicate the relative positions of light sources on the object surfaces. In the figure, the same colored squares across different objects are judged as having the same light sources. In this scene, the green object is selected as the reference object, and the relative positional relationship is determined on this object. Each light source could be classified as one of the four light sources, even though the fluorescent lamps, (2) and (4) had the same spectral power distributions. The classification results are correct for all the candidate light sources. From the detected positional relationship among the multiple light sources, we can predict the relative directions and positions of those light sources on the target objects as follows: Outdoor daylight comes from the left. Two fluorescent lights are at the top front and the top back. LED source exists at the right.

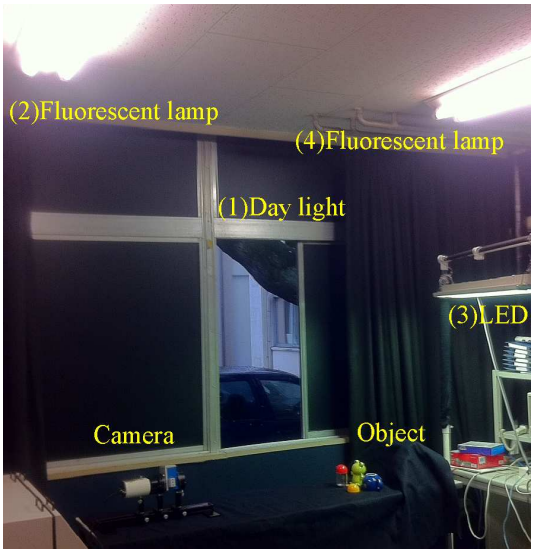

Figure 6. *Experimental scene.*

Figure 7. *Captured image of different objects.*

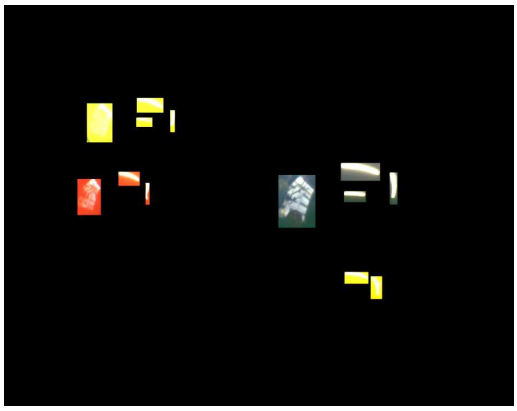

Figure 8. *Detected highlight areas.*

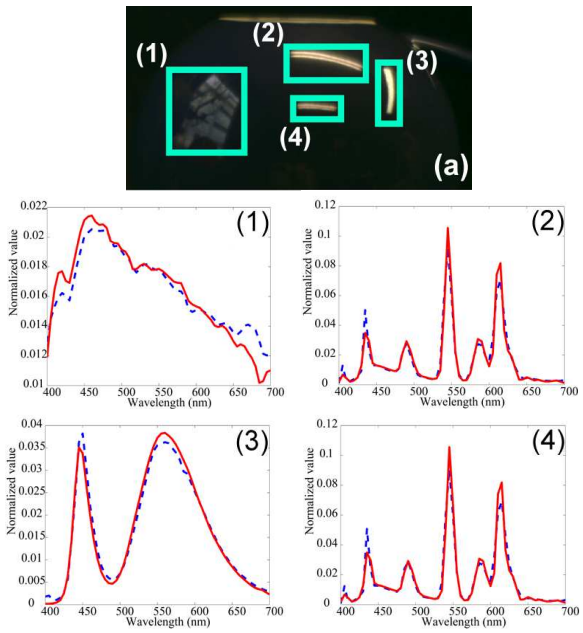

Figure 9. *Close-up of highlights on blue cup and the estimated illuminant spectra.*

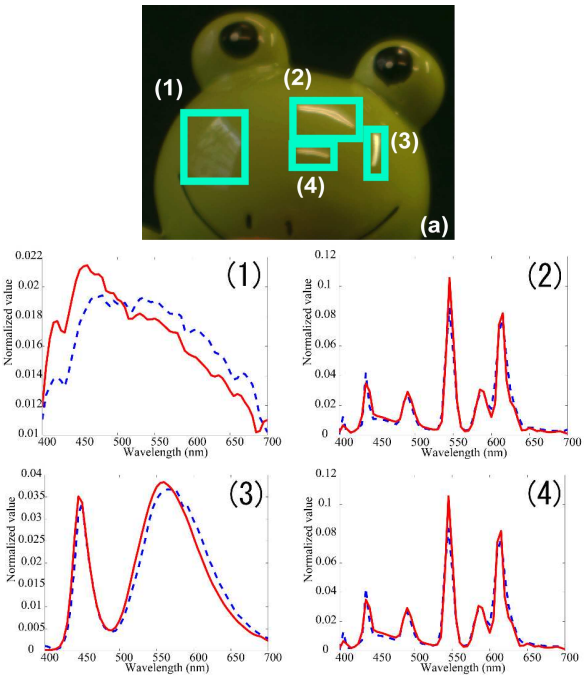

Figure 10. *Close-up of highlights on green object and the estimated illuminant spectra.*

Conclusion

We have proposed a method for estimating the illuminant spectral power distributions and their relative positional relationship of multiple light sources by using only one image of a scene. A multiband camera system was used for capturing spectral images of dielectric objects. First, dielectric object surfaces were segmented into regions with different object colors. The illuminant spectra were estimated from the camera data for highlight areas detected on each surface region. Next, the relative positional relationship of the light sources was predicted based on the set of estimated illuminant spectra on the segmented surface regions. The probabilistic relaxation labeling algorithm was used for this purpose. We have demonstrated experimentally the accuracy of our method, both in detecting the number of light sources and their positional relationship and in estimating their illuminant spectral-power distributions, by examinations on real scenes. The proposed method is applicable even when non-directional ambient light exists in the scene.

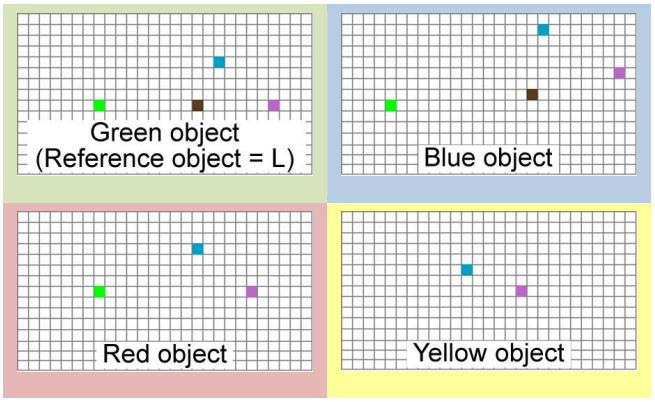

Figure 11. *Classification results on all objects.*

References

[1] A. Tremeau, S. Tominaga. and K. N. Plataniotis, "Color in Image and Video Processing: Most Recent Trends and Future Research Directions, " Eurasip J. Image and Video Processing, 2008, 26 pages. (2008).

[2] S.D. Hordley, "Scene illuminant estimation : Past, present and Future, Color Research and Application," 31, 303 (2006).

[3] S. Tominaga and B.A. Wandell, "Natural Scene Illuminant Estimation Using the Sensor Correlation," Proc. IEEE, 90, 42 (2002).

[4] Y. Wang and D. Samaras, "Multiple Directional Illuminant Estimation from a Single Image," Proc. IEEE Workshop on Color and Photometric Methods in Computer Vision, (2003).

[5] W. Zhou, C. Kambhamettu, "A Unified Framework for Scene Illuminant Estimation," Image Vision Computing, 26, 415 (2006).

[6] K. Hara, K. Nishino and K. Ikeuchi, "Multiple Light Sources and Reflectance Property Estimation based on a Mixture of Spherical Distributions," Proc. ICCV,II, pg. 1627 (2005).

[7] A. Gijsenij, R. Lu and T. Gevers, "Color Constancy for Multiple Light Sources," IEEE Trans. IP, 21, 697 (2012).

[8] A. Rosedfeld, R.A. Hummel and S.W. Zucker, "Scene Labeling by Relaxation Operations," IEEE Trans. SMC, 6, 420 (1976).

Author Biography

Shoji Tominaga received the B.E., M.S., and Ph.D. degrees in electrical engineering from Osaka University, Japan, in 1970, 1972, and 1975, respectively. From 1976 to 2006, he had been with Osaka Electro-Communication University. Since 2006, he is a professor at Graduate School of Advanced Integration Science, Chiba University. During the 1987-1988 academic years he was a Visiting Scholar at the Department of Psychology, Stanford University. He is a fellow of IEEE, IS&T, SPIE and IEICEJ.